Research Article | Vol. 32, No. 22 / 21 Oct 2024 / Optics Express 39460
Optics EXPRESS

# 44-fs, 1-MHz, 70-µJ Yb-doped fiber laser system for high harmonic generation

SEDIGHEH MALEKMOHAMADI,[1,2,*] MIKHAIL PERGAMENT,[1] GABOR KULCSAR,[3] MARCUS SEIDEL,[4] YIZHOU LIU,[1,2] MARVIN EDELMANN,[1,2] MARTIN KELLERT,[1] JELTO THESINGA,[1] CHRISTOPH M. HEYL,[4,5,6] AND FRANZ X. KÄRTNER[1,2]

[1]*Center for Free-Electron Laser Science CFEL, Deutsches Elektronen-Synchrotron DESY, Notkestr. 85, 22607 Hamburg, Germany*
[2]*Department of Physics, Universität Hamburg, Jungiusstr. 9, 20355 Hamburg, Germany*
[3]*Laser Impulse, Wiesenkamp 30, 24226 Heikendorf, Germany*
[4]*Deutsches Elektronen-Synchrotron DESY, Notkestr. 85, 22607 Hamburg, Germany*
[5]*Helmholtz Institute Jena, Fröbelstieg 3, 07743 Jena, Germany*
[6]*GSI Helmholtzzentrum für Schwerionenforschung GmbH, Planckstrasse 1, 64291 Darmstadt, Germany*
[*]*Sedigheh.malek.mohamadi@desy.de*

**Abstract:** We report the development of a robust Yb-doped fiber laser system based on chirped-pulse amplification (CPA), generating 44-fs laser pulses with up to 70-µJ pulse energy at a 1-MHz repetition rate. It consists of a Yb-doped nonlinear polarization evolution (NPE) mode-locked fiber oscillator, a chirped fiber Bragg grating (CFBG) stretcher, a wave-shaper for manipulating the spectrum of the signal, cascaded fiber amplifiers, and two compression units. The output pulse duration of 44 fs for efficient high harmonic generation (HHG) was achieved by a multi-pass multi-plate Herriott-type non-linear compression unit.



## 1. Introduction

Ultrashort pulses with hundreds of microjoule pulse energy, enable various applications such as advanced material processing [1,2], high harmonic generation (HHG) [3,4], attosecond metrology [5], ultrafast spectroscopy [6], and time-resolved coincidence spectroscopy [7]. Specifically, ultrashort pulses in the X-ray and extreme ultraviolet (EUV or XUV) range enable precise and high-resolution measurements [8]. It has been shown, that the required EUV or XUV pulses can be generated using HHG with high pulse energy laser sources. Over the last two decades, detailed investigations of HHG with different sources having different parameters such as peak power or repetition rate have been performed [9]. Titanium-sapphire lasers with high pulse energies and low repetition rates are examples of such sources [10–13]. However, scaling these systems in terms of repetition rate and average power is difficult due to the high thermal load, the lack of direct diode pumping and low optical-to-optical efficiency [14]. In parallel, compact high-power HHG sources based on post-compressed femtosecond ytterbium-doped fiber lasers with high-repetition rate are becoming increasingly popular, especially for time- and angle-resolved photoemission spectroscopy (TR-ARPES) [15,16]. High repetition rate EUV sources have proven to be beneficial for reducing data acquisition times in detecting weak photo electron signals [17]. Fiber-based laser systems have the reputation of being more resistant to thermo-optic problems due to the fiber geometry. The large surface-to-active volume ratio of fibers results in excellent heat dissipation. The beam quality of the guided mode is determined by the design of the fiber core [18,19]. In addition, the complete integration of the lasing process into a waveguide enables compactness, high efficiency and long-term stability. Ytterbium-doped

#538748 https://doi.org/10.1364/OE.538748
Journal © 2024 Received 6 Aug 2024; revised 29 Sep 2024; accepted 2 Oct 2024; published 15 Oct 2024

Optics EXPRESS

optical fibers (YDF) with low quantum defects can have an optical-to-optical efficiency of about 80% and thus low thermal effects [20]. Subsequently, YDF-based laser systems are of particular interest for the generation and amplification of ultrashort high-average power pulses [21]. However, fiber lasers are more severely limited by nonlinear effects, when compared to solid-state lasers, that can lead to pulse deformation and/or damage of the fiber. To lower this limitations by nonlinearity, some approaches have been developed, such as fiber designs with large mode field diameter and a shorter length, resulting in inherently lower nonlinearity [22,23]. Hence, the development of high-power fiber lasers became possible after the invention of double-clad fibers by Snitzer in 1988 [24]. In 2005, Jens Limpert and others arrived at a fiber design known as rod-type photonic crystal fiber (RTF) that exhibits significantly reduced nonlinearity, while allowing for large gain [25]. However, when higher pulse energy is required, the chirped pulse amplification (CPA) technique [26–30] is essential for alleviating the high nonlinearities. In a fiber-based CPA system, pulses are stretched in time to reduce peak power during amplification, thereby minimizing nonlinear effects such as self-phase modulation (SPM) and stimulated Raman scattering (SRS). Despite these techniques, generating high-energy pulses from fiber lasers remains challenging. To achieve this goal, a reduction of pulse repetition rate in conjunction with a larger stretching factor is required. Accordingly, scaling the average power in the following amplifiers results in both high power and high pulse energy.

In this work, we report the development of an ultrafast high-power fiber laser system with a high repetition rate (1 MHz) at 1 μm for HHG to be used in a TR-ARPES setup currently served by a Ti:Sapphire system with a lower repetition rate (10 KHz). The system, based on the CPA technique, generates an average power of up to 70 W at a repetition rate of 1 MHz, allowing a higher signal-to-noise ratio at a shorter data acquisition time. We apply a suitable spectral amplitude filter using a wave shaper to obtain a near transform-limited pulse of about 158 fs. Finally, we shorten the pulse duration to 44 fs with a multi-pass multi-plate cell as a nonlinear compression unit with an excellent output beam quality ($M^2$ value of about 1.2). Our high repetition rate system, with a peak power of up to 1.6 GW, is ideally suited for high harmonic generation (HHG) in time- and angle-resolved photoemission spectroscopy (TR-ARPES) [31].

The system stands out for its combination of high peak power, excellent beam quality, sub-50 fs pulse duration, and high repetition rate, positioning it as one of the leading fiber lasers in its class [4,32–36]. For comparison, Tao Wang et al. [32] developed a Yb-doped fiber amplifier with a pulse energy of 126 μJ at a lower repetition rate (504 kHz) and a longer pulse duration (401 fs), resulting in a lower peak power (207 MW). Likewise, Huanyu Song et al. [34] demonstrated a Yb-fiber laser delivering 24 fs pulses at 1 MHz with 1 μJ pulse energy, yielding approximately 40 times lower peak power. The unique characteristics of our system also make it suitable for a broad range of additional cutting-edge scientific applications, including ultrafast imaging, high-resolution spectroscopy, nonlinear optics, and precision material processing.

## 2. Experimental setup and measurement

Figure 1 shows the constructed high-power fiber laser system consisting of a nonlinear polarization evolution (NPE) mode-locked Yb-doped fiber oscillator as a seeder, a chirped fiber Bragg grating (CFBG) stretcher, a wave-shaper for the signal spectrum and phase shaping, a fiber pre-amplifier chain, a rod-type large pitch Yb-doped fiber (YDF) amplifier, a linear compressor, and a nonlinear compressor.

The mode-locking mechanism of the oscillator is based on the intensity-dependent nonlinear change in the polarization state of the pulse inside the cavity [37–40]. It generates output pulses with a wide output spectrum and is stably mode-locked. The measured pulse duration for the oscillator is around 4.9 ps with a positive chirp and a bandwidth with a full width at half maximum (FWHM) of 19 nm. The output power is around 10 mW with a repetition rate of

Optics EXPRESS

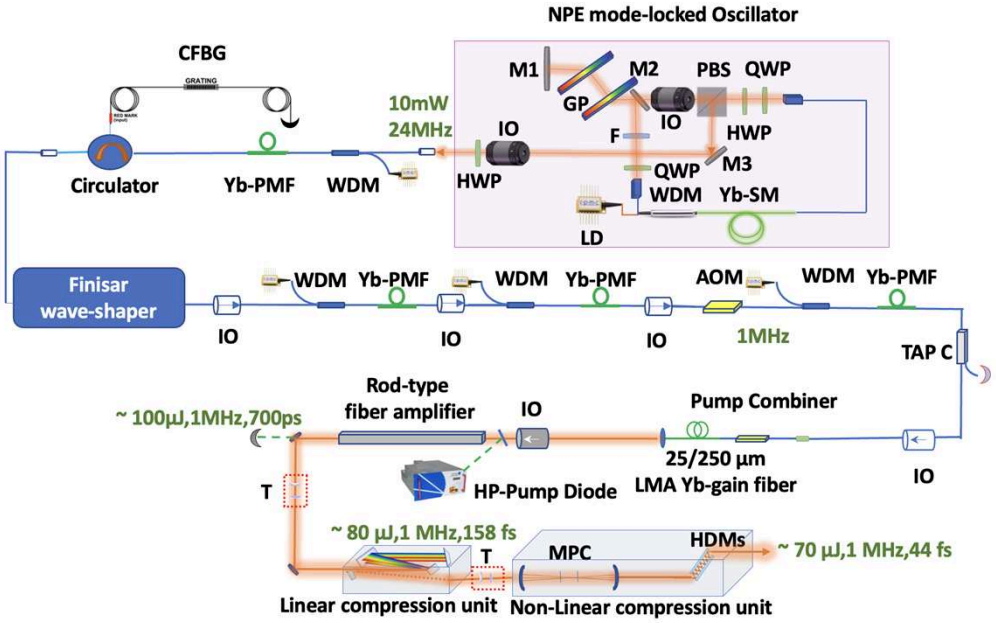


**Fig. 1.** Schematic layout of our system. WDM, wavelength division multiplexer; Yb-SMF, Yb-doped single mode fiber; M, mirror; PMF, polarization maintaining fiber; QWP, quarter-wave plate; HWP, half-wave plate; F, bandpass filter; PBS, polarization beam splitter; GP, grating pair; LD, laser diode; CFBG, chirped fiber Bragg grating; IO, isolator; AOM, acousto-optic modulator; TAP C, tap coupler; LMA, large mode area fiber; HP, high-power; T, telescope; MPC, multi-pass cell; HDM, highly-dispersive mirror.

24 MHz. The seed source is a self-mode-locking oscillator that has reliably maintained mode-locked over an extended period without requiring any additional adjustments. This reliability is crucial for long-term stability and efficient performance of the overall system. However, since non-polarization-maintaining (non-PM) single-mode fibers are used in the oscillator, the output spectrum is somewhat sensitive to ambient noise and temperature fluctuations. To mitigate these effects, we have shielded the entire system, ensuring a well-controlled environment that minimizes these instabilities.

The output signal from the NPE-oscillator is coupled into a highly-doped polarization maintaining (PM) YDF pre-amplifier (gain length of about 40 cm and pump power of 100 mW) to overcome the 40% loss of the following stretcher and circulator. The stretcher is a chirped fiber Bragg grating (CFBG) with 30.1 $ps^2$ group delay dispersion and -0.4 $ps^3$ third-order dispersion covering a 22-nm wide spectrum and stretches the pulse duration to approximately 1 ns. The CFBG was designed to mitigate the nonlinearity of the whole system and compensate for the dispersion of a Treacy compressor and its upstream optical components in the system. We use a wave-shaper (Finisar Wave-Shaper 1000A) to shape the spectrum of the stretched signal into a nearly parabolic spectrum. Pulse pedestals due to SPM are avoided for a parabolic shaped pulse spectrum at the output of the amplifiers [29,30,41]. Therefore, we apply a parabolic filter in the frequency domain according to:

$$F(\nu) = 1 - \left( \frac{\sqrt{2}(\nu - \nu_0)}{\Delta\nu_{FWHM}} \right)^2 \tag{1}$$

Optics EXPRESS

where $\nu_0$ denotes the central frequency and $\Delta\nu_{FWHM}$ the bandwidth at the full width of half maximum (FWHM). In practice, $\Delta\nu_{FWHM}$ is chosen large enough to alleviate the gain narrowing effect on the spectrum in the next amplifier chain and maximize the FWHM spectral width of the output signal. Figure 2(a) shows the output spectrum and up-chirped pulse (inset) of the oscillator. Figure 2(b) indicates the spectrum before and after filtering for $\Delta\nu_{FWHM} = 9\ THz$, and a central wavelength of 1030 nm. There are small fluctuations in the amplitude after filtering due to the slight change in the seed signal because of environmental instabilities. To mitigate this, we enclose the entire system in a shielded, controlled environment that reduces instabilities, ensuring a more consistent and reliable output spectrum despite external disturbances. A pedestal-free nearly transform-limited pulse is generated by the system for this filter shape in spectral amplitude, which is explained later.

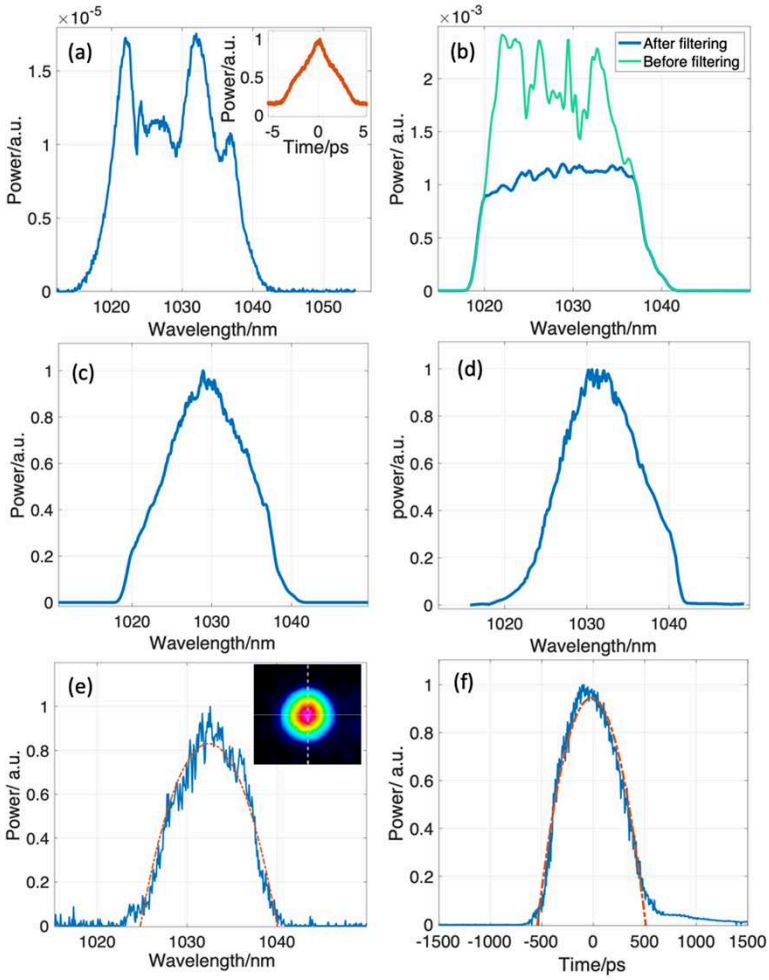


**Fig. 2.** (a) The oscillator output spectrum and pulse shape (inset). (b) The spectrum before and after filtering by the Finisar wave-shaper. (c) The spectrum after TAP C. (d) The spectrum after LMA fiber amplifier. (e)The output spectrum (measured with a higher resolution in comparison with others), the inset is the rod-type amplifier (RTA) beam profile with $M^2$ of 1.1 and (f) the pulse duration after RTA measured with an Agilent Technologies Sampling Oscilloscope. Red dashed curves are parabolic fits.

Optics EXPRESS

The wave shaper (with up to 6.5 dB insertion loss) is followed by two more preamplifiers with highly doped PM-YDF (gain length of 35 cm and the pump power of 300 mW for the preamplifier 2, gain length of 50 cm and the pump power of 450 mW for the preamplifier 3) to increase the wave-shaper output and overcome the loss of a fiber-coupled acousto-optic modulator (AOM) used for pulse picking. The AOM reduces the pulse repetition rate from 24 MHz to 1 MHz, which helps to achieve higher pulse energy in the following amplifiers. The fourth pre-amplifier (gain length of 40 cm and the pump power of 450 mW) reaches an output power up to 400 mW, which is appropriate for saturation of the following large mode area (LMA) fiber amplifier (25/250 µm LMA-YDF). The higher-order modes in the LMA fiber were suppressed by coiling of the fiber to a diameter of 60 mm. Up to 6 W output power can be achieved from this amplifier, enough to also saturate the final amplifier with the rod-type fiber (AEROGAIN-ROD 2.1, signal average power $\leq$ 100 $W$). Figures 2(c) and 2(d) show the evolution of the spectrum, measured after the tap coupler and the LMA amplifier, respectively. We installed a free space high-power isolator before the rod-type amplifier (RTA) to block the backward amplified spontaneous emission (ASE) and eventual back reflections. Then the signal is coupled into the RTA utilizing two adjustment mirrors and a coupling lens. The beam quality ($M^2$) at optimal mode coupling is measured to be about 1.1 and a picture of the near field is shown in the inset of Fig. 2(e). The RTA is pumped with an industrial high-power diode laser (Laser-Line LDM-500). With a signal power of 5 W, an average power of up to 100 W can be achieved with this rod-type fiber. The shape of the RTA output spectrum (2 (e)) and the stretched pulse (2 (f)) comes close to a parabolic fit. Due to the linear chirp that SPM applies to an output parabolic pulse, the pedestal in the temporal signal after the linear compressor is effectively suppressed. We design and construct a Treacy compressor using a pair of multilayer dielectric reflection gratings with a groove density of 1760l/mm and a Littrow angle of 65.01° (diffraction efficiency > 95%) as the linear compression unit with a loss of 13%.

Figure 3(a) shows the optimum compressed amplifier output pulses in the time domain, when no spectral shaping is performed. A strong pedestal can be seen in the compressed pulse. We suppress the pedestal by using near-parabolic spectral filter. A pedestal-free near transform-limited pulse (Fig. 3(b)) is achieved when the RTA output spectrum is formed into a parabola (Fig. 2(c)). The measured pulse duration is about 158 fs. It is close to the calculated transformation-limited pulse duration of the output spectrum, which is about 152 fs. A pedestal-free pulse enhances the efficiency of spectrum broadening within the multi-pass cell (MPC, explained in the next section), leading to shorter pulses with minimal pedestal at the final output of the system.

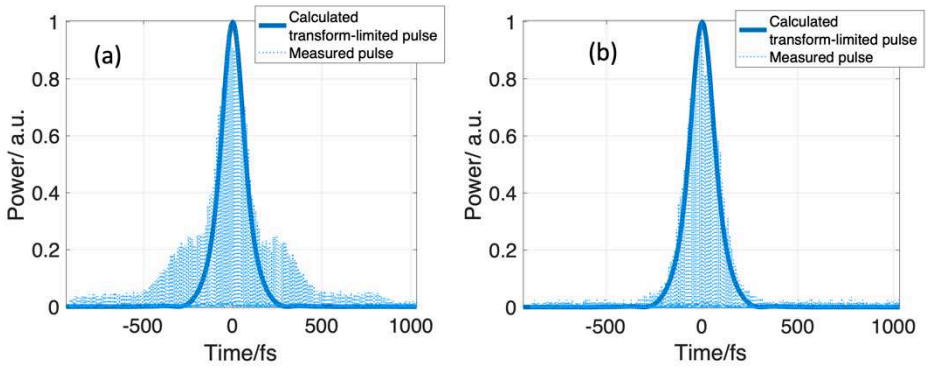


**Fig. 3.** Compressed pulse duration measured by second-harmonic autocorrelation with $sech^2$ fit.: (a) with no spectrum manipulation, (b) with the introduced parabolic spectrum filter using the Finisar wave-shaper.

Optics EXPRESS

A shorter pulse duration is required to increase peak power for efficient high harmonic generation and improved temporal resolution in pump-probe experiments. Direct generation of pulses with duration shorter than 100 fs at high power is not possible from Yb-doped fiber amplifier systems due to the limited gain bandwidths of the laser medium and the resulting gain narrowing effect [42]. Nonlinear pulse compression is a possible approach to achieve shorter pulse durations that can be used with high-power lasers. In this method, the spectrum of the laser pulse is broadened by SPM as it propagates through a $\chi^{(3)}$ nonlinear medium. A temporally compressed pulse can then be attained by compensating for the chirp of the broadened pulse spectrum with grating pair compressor or dispersive mirrors. Propagation of ultrashort pulses through solid core fibers [43], hollow-core photonic crystal fibers [44], gas-filled capillaries [45], bulk media, and multi-pass cells [42] are some of the various techniques applied for nonlinear spectral broadening. Here, we use a Herriott-type multi-pass cell (MPC) compressor with bulk dielectric plates for nonlinear pulse compression in the range of 10-100 μJ-pulses first reported in [42]. Pulses accumulate a B integral $\ll\pi$ each time they pass through the nonlinear medium. In this procedure, pulses even exceeding the peak power for self-focusing can be nonlinearly broadened, and the degradation of the beam quality is mitigated due to the use of thin plates [46]. This approach offers unprecedented robustness and scalability in average power [42].

An MPC typically consists of two concave mirrors oriented as an optical cavity to create transverse eigenmodes and preserve the q-parameter of a Gaussian beam matched to the cell eigenmode (see Fig. 4(a)) [47,48]. The laser beam is matched to the cavity mode with the help of a telescope to ensure identical beam properties each time it passes through the cell. It is then coupled into the MPC by a small pick-off mirror [2,49]. After a certain number of round trips (16 round trips in our case), the spectrally broadened output beam is coupled out of the cell [50]. The beam is subsequently collimated, and the pulses are compressed using a chirped mirror compressor.

The B integral is a measure of spectral broadening [2,51]. We simulated the cell length, the beam radius on the mirrors, the position of the plates based on their thicknesses, the beam waist and the position of the focal plane in the MPC using the method introduced in Ref. [46,52,53] to obtain a sufficient amount of B-integral. For the MPC with N = 16 round trips, a cell length of 366 mm results in the higher B-integral without the risk of damaging the surfaces. Here, we used a dual-plate multi-pass cell defined by two curved mirrors with radius of curvature of 200 mm (HR > 99.99%, $|GDD|<20 fs^2$) and two internal fused silica plates with a thickness of 1 mm (AR < 0.2%). The $M^2$ factor of the input beam is measured as $M_x^2 \times M_y^2$ : 1.10 × 1.06 with the $M^2$-measurement device Spiricon-$M^2$-200s. As is depicted in the inset of Fig. 4(a) the beam profile is near-diffraction-limited.

We employed a compressor made by chirped-mirrors with group delay dispersion (GDD) of -200 $fs^2$ and a negligible TOD per bounce to compress the spectrally broadened pulses with 16 bounces. The output of the nonlinear compressor is analyzed using an optical spectrum analyzer (OSA) and a second harmonic FROG-device as depicted in Fig. 4(b) and (c). The spectrally broadened pulse whose spectrum is monitored with the OSA, and the retrieved power spectra by the FROG are displayed in Fig. 4(b). The modulation in the measured spectrum results from the strong self-phase modulation. The discrepancy between the measured and retrieved spectra arises from two main factors: limitations in the retrieval algorithm (restricted by a maximum grid size of 256 × 256) and the constraints of the FROG device in capturing the full details of our strongly modulated spectrum. The FROG system with the available crystal has a spectral measurement resolution of about 5 nm, which is insufficient to resolve the finer spectral features of our signal. Consequently, the device is unable to accurately reproduce the full spectral detail, leading to significant differences between the measured and retrieved spectra. The measured pulse duration (44 fs at FWHM), as well as the calculated transform-limited (TL) pulse corresponding to the

Optics EXPRESS

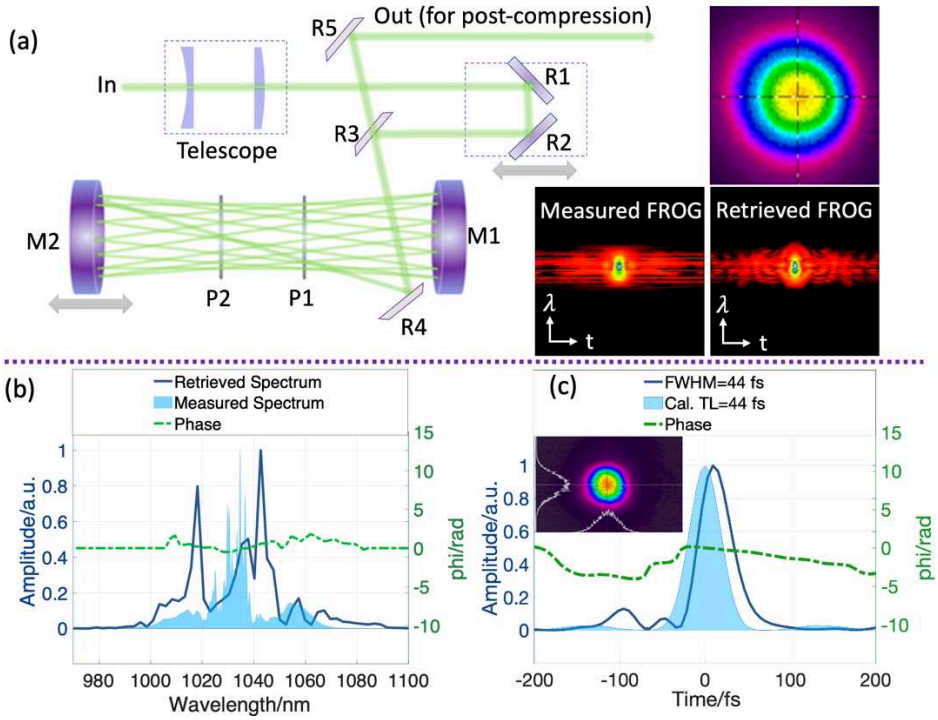


**Fig. 4.** (a) Spectral broadening with a dual-plate MPC; M, curved mirror; R, reflective flat mirror; P, plate. The inset shows the MPC input beam profile, the measured FROG, and the retrieved FROG traces. (b) The measured and retrieved power spectra and phase in the frequency domain, (c) The FROG measurement, calculated transform-limited pulse (Cal. TL) and the phase in the time domain, the inset depicts the output beam profile.

measured spectrum, are shown in Fig. 4(c). The small pedestal in the pulse is because of the nonlinear phase shift induced by SPM that is not compensated by the chirped mirrors.

As can be observed, we could achieve a FWHM pulse duration of 44 fs with about 10% of the pulse energy in the pedestal after post-compression.

The MPC has a measured throughput efficiency of 86%. We measured an $M^2$ value of about 1.2 for the output beam profile displayed in the inset of Fig. 4(c). The nearly Gaussian beam shape underlines the advantages of this approach for spectral broadening compared to single-pass propagation of the pulse in the critical self-focusing regime, which leads to detrimental spatial effects on the beam profile [42].

## 3. Conclusion

In this work, we demonstrate a robust, high-power, high-repetition-rate fiber laser system for high-harmonic generation applications. We control the final temporal pulse shape and avoid pulse pedestal formation in the CPA fiber amplifier system delivering 158-fs, 80-μJ pulses at 1 MHz repetition rate by spectral amplitude shaping. The pulse duration is close to its transform limited value of 152 fs. Using a Herriott-type multi-pass double-plate cell, we achieve sub-50 femtosecond pulses with nearly Gaussian beam profile with beam quality factor $M^2 = 1.2$. This final 1-MHz Yb-doped fiber laser system delivers 70-μJ, 44-fs pulses with a peak power of up to 1.6 GW suitable for a HHG system for a TR-ARPES setup. This allows an improvement of the acquisition rate for the already existing TR-ARPES setup using a 10 kHz Ti:sapphire laser

Optics EXPRESS

system by at least two orders of magnitude. The next development step will be to increase the repetition rate to 2 MHz at the same pulse energy.

**Funding.** Deutsche Forschungsgemeinschaft (Cluster of Excellence, CUI:Advanced Imaging of Matter, EXC 2056 project ID 390715994); Helmholtz Association (Deutsches Elektronen-Synchrotron).

**Disclosures.** The authors declare no conflicts of interest.

**Data availability.** Data underlying the results presented in this paper are not publicly available at this time but may be obtained from the authors upon reasonable request.

## References

1. K. Sugioka and Y. Cheng, "Ultrafast lasers—reliable tools for advanced materials processing," Light: Sci. Appl. **3**(4), e149 (2014).
2. A.-L. Viotti, M. Seidel, E. Escoto, *et al.*, "Multi-pass cells for post-compression of ultrashort laser pulses," Optica **9**(2), 197–216 (2022).
3. S. Hädrich, J. Rothhardt, M. Krebs, *et al.*, "Single-pass high harmonic generation at high repetition rate and photon flux," J. Phys. B: At., Mol. Opt. Phys. **49**(17), 172002 (2016).
4. J. S. Feehan, J. H. V. Price, T. J. Butcher, *et al.*, "Efficient high-harmonic generation from a stable and compact ultrafast Yb-fiber laser producing 100 μJ, 350 fs pulses based on bendable photonic crystal fiber," Appl. Phys. B **123**(1), 43 (2017).
5. I. Orfanos, I. Makos, I. Liontos, *et al.*, "Attosecond pulse metrology," APL Photonics **4**(8), 080901 (2019).
6. D. J. Richardson, J. Nilsson, and W. A. Clarkson, "High power fiber lasers: current status and future perspectives [Invited]," J. Opt. Soc. Am. B **27**(11), B63–B92 (2010).
7. C. L. Arnold, S. Mikaelsson, J. Vogelsang, *et al.*, "A high-repetition rate attosecond pulse source for time-resolved coincidence spectroscopy and nanoscale imaging," in *Conference on Lasers and Electro-Optics (2021)*, Paper FTu2O.2 (Optica Publishing Group, 2021), p. FTu2O.2.
8. W. Eschen, L. Loetgering, V. Schuster, *et al.*, "Material-specific high-resolution table-top extreme ultraviolet microscopy," Light: Sci. Appl. **11**(1), 117 (2022).
9. C. M. Heyl, C. L. Arnold, A. Couairon, *et al.*, "Introduction to macroscopic power scaling principles for high-order harmonic generation," J. Phys. B: At., Mol. Opt. Phys. **50**(1), 013001 (2017).
10. H. Coudert-Alteirac, H. Dacasa, F. Campi, *et al.*, "Micro-focusing of broadband high-order harmonic radiation by a double toroidal mirror," Appl. Sci. **7**(11), 1159 (2017).
11. S. Kühn, M. Dumergue, S. Kahaly, *et al.*, "The ELI-ALPS facility: the next generation of attosecond sources," J. Phys. B: At., Mol. Opt. Phys. **50**(13), 132002 (2017).
12. C. Kleine, M. Ekimova, G. Goldsztejn, *et al.*, "Soft x-ray absorption spectroscopy of aqueous solutions using a table-top femtosecond soft x-ray source," J. Phys. Chem. Lett. **10**(1), 52–58 (2019).
13. B. Shan, A. Cavalieri, and Z. Chang, "Tunable high harmonic generation with an optical parametric amplifier," Appl. Phys. B **74**(S1), s23–s26 (2002).
14. J. Limpert, F. Roeser, T. Schreiber, *et al.*, "High-power ultrafast fiber laser systems," IEEE J. Sel. Top. Quantum Electron. **12**(2), 233–244 (2006).
15. J. Boullet, Y. Zaouter, J. Limpert, *et al.*, "High-order harmonic generation at a megahertz-level repetition rate directly driven by an ytterbium-doped-fiber chirped-pulse amplification system," Opt. Lett. **34**(9), 1489–1491 (2009).
16. S. Hädrich, A. Klenke, J. Rothhardt, *et al.*, "High photon flux table-top coherent extreme-ultraviolet source," Nat. Photonics **8**(10), 779–783 (2014).
17. H. Zhang, T. Pincelli, C. Jozwiak, *et al.*, "Angle-resolved photoemission spectroscopy," Nat. Rev. Methods Primer **2**(1), 54 (2022).
18. S. Poole, D. Payne, R. Mears, *et al.*, "Fabrication and characterization of low-loss optical fibers containing rare-earth ions," J. Light. Technol **4**(7), 870–876 (1986).
19. Y. H. Lim, G. Tan, and S.-L. Chua, "Effective Single-mode Fibers with Large Mode Areas Through Intermodal-coupling," Procedia Eng **140**, 49–56 (2016).
20. L. Goldberg, J. P. Koplow, and D. A. V. Kliner, "Highly efficient 4-W Yb-doped fiber amplifier pumped by a broad-stripe laser diode," Opt. Lett. **24**(10), 673–675 (1999).
21. R. Paschotta, J. Nilsson, A. C. Tropper, *et al.*, "Ytterbium-doped fiber amplifiers," IEEE J. Quantum Electron **33**(7), 1049–1056 (1997).
22. D. Gloge, "Weakly guiding fibers," Appl. Opt **10**(10), 2252–2258 (1971).
23. J. P. Koplow, D. A. V. Kliner, and L. Goldberg, "Single-mode operation of a coiled multimode fiber amplifier," Opt. Lett. **25**(7), 442–444 (2000).
24. E. Snitzer, H. Po, F. Hakimi, *et al.*, "Double clad, offset core ND fiber laser," in *Optical Fiber Sensors (1988)*, Paper PD5 (Optica Publishing Group, 1988), p. PD5.
25. J. Limpert, N. Deguil-Robin, I. Manek-Hönninger, *et al.*, "High-power rod-type photonic crystal fiber laser," Opt. Express **13**(4), 1055–1058 (2005).
26. C. Rolland and P. B. Corkum, "Compression of high-power optical pulses," J. Opt. Soc. Am. B **5**(3), 641–647 (1988).

Optics EXPRESS


27. D. Anderson, M. Desaix, M. Karlsson, *et al.*, "Wave-breaking-free pulses in nonlinear-optical fibers," J. Opt. Soc. Am. B **10**(7), 1185–1190 (1993).
28. K. Tamura and M. Nakazawa, "Pulse compression by nonlinear pulse evolution with reduced optical wave breaking in erbium-doped fiber amplifiers," Opt. Lett. **21**(1), 68–70 (1996).
29. A. Chong, H. Liu, B. Nie, *et al.*, "Pulse generation without gain-bandwidth limitation in a laser with self-similar evolution," Opt. Express **20**(13), 14213–14220 (2012).
30. M. E. Fermann, V. I. Kruglov, B. C. Thomsen, *et al.*, "Self-similar propagation and amplification of parabolic pulses in optical fibers," Phys. Rev. Lett **84**(26), 6010–6013 (2000).
31. S. Malek Mohamadi Faradonbeh, "Ultrafast, high repetition rate, high-power Yb-doped fiber laser systems," doctoralThesis, Staats- und Universitätsbibliothek Hamburg Carl von Ossietzky (2023).
32. T. Wang, B. Ren, C. Li, *et al.*, "Monolithic tapered Yb-doped fiber chirped pulse amplifier delivering 126 μJ and 207 MW femtosecond laser with near diffraction-limited beam quality," Front. Optoelectron **16**(1), 30 (2023).
33. C. Gao, Y. Gui, Y. Wang, *et al.*, "Monolithic Yb-doped femtosecond fiber laser with >300 W average power," IEEE Photonics J **15**(4), 1–5 (2023).
34. H. Song, B. Liu, Y. Li, *et al.*, "Practical 24-fs, 1-μJ, 1-MHz Yb-fiber laser amplification system," Opt. Express **25**(7), 7559–7566 (2017).
35. "Jasper X0: high power femtosecond fiber laser 1030 nm: Fluence," https://www.iberoptics.com/en/femtosecond-fs-pulsed-lasers/fluence_high-power-femtosecond-laser-4400.html.
36. F. Roeser, J. Rothhard, B. Ortaç, *et al.*, "131 W 220 fs fiber laser system," Opt. Lett. **30**(20), 2754–2756 (2005).
37. M. E. Fermann, M. J. Andrejco, Y. Silberberg, *et al.*, "Passive mode locking by using nonlinear polarization evolution in a polarization-maintaining erbium-doped fiber," Opt. Lett. **18**(11), 894–896 (1993).
38. K. Tamura, H. A. Haus, and E. P. Ippen, "Self-starting additive pulse mode-locked erbium fibre ring laser," Electron. Lett **28**(24), 2226–2228 (1992).
39. M. Edelmann, M. M. Sedigheh, Y. Hua, *et al.*, "Large-mode-area soliton fiber oscillator mode-locked using NPE in an all-PM self-stabilized interferometer," Appl. Opt **62**(7), 1672–1676 (2023).
40. J. Kim and Y. Song, "Ultralow-noise mode-locked fiber lasers and frequency combs: principles, status, and applications," Adv. Opt. Photonics **8**(3), 465–540 (2016).
41. D. N. Schimpf, J. Limpert, and A. Tünnermann, "Controlling the influence of SPM in fiber-based chirped-pulse amplification systems by using an actively shaped parabolic spectrum," Opt. Express **15**(25), 16945–16953 (2007).
42. J. Schulte, T. Sartorius, J. Weitenberg, *et al.*, "Nonlinear pulse compression in a multi-pass cell," Opt. Lett. **41**(19), 4511–4514 (2016).
43. C. Jocher, T. Eidam, S. Hädrich, *et al.*, "Sub 25 fs pulses from solid-core nonlinear compression stage at 250 W of average power," Opt. Lett. **37**(21), 4407–4409 (2012).
44. F. Emaury, C. J. Saraceno, B. Debord, *et al.*, "Efficient spectral broadening in the 100-W average power regime using gas-filled kagome HC-PCF and pulse compression," Opt. Lett. **39**(24), 6843–6846 (2014).
45. S. Hädrich, M. Kienel, M. Müller, *et al.*, "Energetic sub-2-cycle laser with 216 W average power," Opt. Lett. **41**(18), 4332–4335 (2016).
46. M. Seidel, P. Balla, C. Li, *et al.*, "Factor 30 pulse compression by hybrid multipass multiplate spectral broadening," Ultrafast Sci. **2022**, 1–10 (2022).
47. D. Herriott, H. Kogelnik, and R. Kompfner, "Off-axis paths in spherical mirror interferometers," Appl. Opt **3**(4), 523–526 (1964).
48. A. M. Kowalevicz, A. Sennaroglu, A. T. Zare, *et al.*, "Design principles of q-preserving multipass-cavity femtosecond lasers," J. Opt. Soc. Am. B **23**(4), 760–770 (2006).
49. P. Russbueldt, T. Mans, J. Weitenberg, *et al.*, "Compact diode-pumped 1.1 kW Yb:YAG Innoslab femtosecond amplifier," Opt. Lett. **35**(24), 4169–4171 (2010).
50. M. Kaumanns, V. Pervak, D. Kormin, *et al.*, "Multipass spectral broadening of 18 mJ pulses compressible from 1.3 ps to 41 fs," Opt. Lett. **43**(23), 5877–5880 (2018).
51. S. C. Pinault and M. J. Potasek, "Frequency broadening by self-phase modulation in optical fibers," J. Opt. Soc. Am. B **2**(8), 1318–1319 (1985).
52. A.-K. Raab, M. Seidel, C. Guo, *et al.*, "Multi-gigawatt peak power post-compression in a bulk multi-pass cell at a high repetition rate," Opt. Lett. **47**(19), 5084–5087 (2022).
53. A.-L. Viotti, C. Li, G. Arisholm, *et al.*, "Few-cycle pulse generation by double-stage hybrid multi-pass multi-plate nonlinear pulse compression," Opt. Lett. **48**(4), 984–987 (2023).